International Journal of Fracture 27 (1985) 229–243.

Computational methods based on an energy integral in dynamic fracture

T. NAKAMURA, C.F. SHIH and L.B. FREUND

Division of Engineering, Brown University, Providence, RI 02912, USA

(Received September 1, 1984)

Abstract

Developments in the use of the crack tip energy flux integral in computational dynamic fracture mechanics over the past few years are reviewed. An expression for the crack tip energy flux in terms of near tip mechanical fields which is valid for general material response is derived. It is then demonstrated that certain useful energy integrals may be extracted from the general result by invoking the appropriate characterization of material response. Several alternative representations of energy flux in the form of integrals over some finite region around the crack tip are presented and compared with a view toward implementation in finite element simulation studies.

1. Introduction

The first crack tip contour integral expression for elastodynamic energy release rate was proposed by Atkinson and Eshelby [1], who argued that the form for dynamic growth should be the same as for quasi-static growth with the elastic energy density replaced by the total mechanical energy density, that is, the elastic energy plus the kinetic energy. The equivalent integral expression for dynamic energy release rate in terms of crack tip stress and deformation fields was subsequently derived directly from the field equations of elastodynamics by Kostrov and Nikitin [2] and by Freund [3]. They enforced an instantaneous energy rate balance for the time-dependent volume of material bounded by the outer boundary of the solid, the crack faces, and small loops surrounding each moving crack tip and translating with it. By application of Reynold's transport theorem [4] and the divergence theorem an expression for crack tip energy flux in the form of an integral of field quantities along the crack tip loop was obtained. A result which is applicable to a much broader range of material response and which contains the earlier elastodynamic result as a special case is derived here, with an observation made by Eshelby [5] on the form of the equations of motion as a point of departure. A similar result has also been obtained by Willis [6].

In the analysis of dynamic crack phenomena by means of computational methods, such as the finite element method, a fundamental difficulty is encountered in efforts to compute values of the crack tip energy flux versus time or amount of crack growth. The difficulty arises from the fact that, on the one hand, the crack tip energy flux is defined in terms of the values of field quantities for points arbitrarily close to the crack tip while, on the other hand, it is precisely for points near the crack tip for which the accurate calculation of field quantities is most difficult. In an effort to circumvent this difficulty, finite domain integrals have been introduced for the computation of dynamic energy release rate by Kishimoto, Aoki and Sakata [7,8], by Atluri [9], and by Nishioka and Atluri [10–12].

The purpose here is to review developments in this area over the past few years. First, an expression for crack tip energy flux which is valid for general material response is derived in a direct manner. While a variety of seemingly different path-independent energy integrals have been proposed in recent years, each may be extracted from this general result by invoking the appropriate restrictions on material response and crack tip motion. Several alternate expressions for the energy flux integral are obtained from the general result by application of the divergence theorem over some part of the fracturing solid and these expressions are compared, with a view toward implementation in finite element simulations. For the illustrations based on elastodynamic crack growth, exact solutions are available to test the computed quantities. In the case of elastic-plastic response, on the other hand, no exact solutions exist to provide a basis for comparison.

2. The crack tip energy flux integral

In the absence of body forces, the equation of motion in terms of cartesian components of stress σ_{ij} and displacement u_i is

$$\frac{\partial \sigma_{ij}}{\partial x_j} - \rho \frac{\partial^2 u_i}{\partial t^2} = 0, \tag{2.1}$$

where ρ is mass density. If the inner product of (2.1) with the particle velocity $\partial u_i/\partial t$ is formed, then the resulting equation may be written in the form

$$\frac{\partial}{\partial x_j}\left(\frac{\partial u_i}{\partial t}\sigma_{ij}\right) - \frac{\partial}{\partial t}(U+T) = 0, \tag{2.2}$$

where U is the stress work density and T is the kinetic energy density, namely, at any material point,

$$U = \int_0^t \sigma_{ij} \frac{\partial^2 u_i}{\partial t' \partial x_j} \mathrm{d}t' \qquad T = \tfrac{1}{2}\rho \frac{\partial u_i}{\partial t}\frac{\partial u_i}{\partial t}. \tag{2.3}$$

Equation (2.2) is a differential form of the work balance principle which is valid for any material response.

If the time coordinate is now given the same status as a spatial coordinate, then (2.2) is the requirement that a certain vector expression is divergence free in a particular "volume" of space-time, that is, it represents a mechanical conservation law. Thus, if the divergence theorem is applied over this volume, the result is that the integral over the bounding surface of this volume of the inner product of the divergence free vector with the surface unit normal vector vanishes. For definiteness, consider a two-dimensional body which contains an extending crack and bounded by a curve C (attached to arbitrary material particles). The plane of the body is the x_1, x_2-plane, the crack plane is $x_2 = 0$ and crack growth is along the x_1-axis. The instantaneous crack tip speed is v. A small contour Γ begins on one traction free face of the crack, surrounds the tip, and ends on the opposite traction free face. This crack tip contour is fixed in size and orientation with respect to the crack tip coordinates as the crack grows. Consider the volume in the x_1, x_2, t-space that is bounded by the planes $t = t_1$ and $t = t_2$, where t_1 and t_2 are arbitrary times, by the right cylinder swept out by C between the two times, by the planes swept out by the crack faces between the two times, and by the tubular surface swept out by the small contour Γ as the crack advances in the x_1-direction with increasing time. For this particular choice of surface, the surface integral which results from application of the

divergence theorem and Reynold's transport theorem is

$$\int_{t_1}^{t_2}\int_C \sigma_{ij}n_j\frac{\partial u_i}{\partial t}\mathrm{d}C\mathrm{d}t = \left[\int_{A(t)}(U+T)\mathrm{d}A\right]_{t_1}^{t_2} + \int_{t_1}^{t_2}\int_\Gamma\left(\sigma_{ij}n_j\frac{\partial u_i}{\partial t}+(U+T)vn_1\right)\mathrm{d}\Gamma\mathrm{d}t, \tag{2.4}$$

where $A(t)$ is the cross-section of the above-mentioned volume on any plane $t =$ constant, n_i is a unit vector that is normal to C or Γ in any plane $t =$ constant and that points away from the crack tip, and vn_1 is the instantaneous velocity of any point on Γ in the direction of n_i at this point.

The term on the left side of (2.4) is the total work done on the body in the time interval of interest, and the first term on the right side is the increase in internal energy during the same time. Consequently, the last term in (2.4) is the total energy lost from the body due to flux through Γ during the interval $t_1 \le t \le t_2$. Because this time interval is completely arbitrary, it follows immediately that the crack tip line integral

$$F(\Gamma) = \int_\Gamma\left(\sigma_{ij}n_j\frac{\partial u_i}{\partial t}+(U+T)vn_1\right)\mathrm{d}\Gamma \tag{2.5}$$

is the instantaneous rate of energy flow out of the body through Γ. The interpretation of the terms in (2.5) is straightforward. The first term is the rate of work of the material outside of Γ on the material inside of Γ. If the curve were a material line, then this would be the only contribution to the energy flux. The curve is moving through the material, however, and the second term in (2.5) represents the contribution to the energy flux due to the flux of material.

The dynamic energy release rate $\mathscr{G}$, that is, the energy released from the body per unit crack advance, is defined as the limiting value of $F(\Gamma)/v$ as the contour Γ is shrunk onto the crack tip. In order for this concept to have any fundamental significance, it is necessary that the result of the limiting process be independent of the actual shape of Γ as its size becomes vanishingly small. Surely F itself is not path-independent in general, as can be seen by means of a direct check. Consider the closed path formed by two crack tip contours Γ_1 and Γ_2, and by the segments of the crack faces that connect the ends of these contours. Application of the divergence theorem to the energy flux integral for this entire closed path leads to the result that

$$F(\Gamma_2) - F(\Gamma_1) = \int_{A_{12}}\left[\left(\frac{\partial U}{\partial t}+v\frac{\partial U}{\partial x_1}\right)+\rho\frac{\partial u_i}{\partial t}\left(\frac{\partial^2 u_i}{\partial t^2}+v\frac{\partial^2 u_i}{\partial t\partial x_1}\right)\right]\mathrm{d}A, \tag{2.6}$$

where A_{12} is the area within the closed path. An equivalent expression for linearly elastic response appears as (14) in [3]. For points very close to the crack tip, it is evident that F will indeed be path-independent (provided that the singularities in field quantities are such that the integral defining F exists near the crack tip) in the limit as Γ shrinks onto the tip if u_i is smooth enough for its second derivatives to exist and if

$$\frac{\partial f}{\partial t}+v\frac{\partial f}{\partial x_1} = o\left(\frac{\partial f}{\partial x_1}\right) \qquad \text{as} \quad r\to 0^+, \tag{2.7}$$

where f is any field variable and r is the radial distance from the moving crack tip. It is noted that the right side of (2.6) is zero by definition for steady-state crack growth problem formulations, so that (2.5) provides a path-independent integral for this class of problems for any type of material response.

If (2.7) is assumed to hold for arbitrary crack tip motion under dynamic conditions, then $\partial u_i/\partial t$ may be replaced by $-v\partial u_i/\partial x_1$ in (2.5) so that

$$\mathscr{G} = \lim_{\Gamma\to 0}\int_\Gamma\left((U+T)n_1-\sigma_{ij}n_j\frac{\partial u_i}{\partial x_1}\right)\mathrm{d}\Gamma. \tag{2.8}$$

Any difference between $\partial u_i/\partial t$ and $-v\partial u_i/\partial x_1$ which is less singular than $\partial u_i/\partial x_1$ cannot contribute to the value of $\mathcal{G}$. The general result (2.8) underlies virtually all crack tip energy integrals that have been defined and applied in fracture mechanics, in the sense that each may be derived from (2.8) by invoking the appropriate restrictions on material response (through U) and on crack tip motion. Some illustrations and applications are cited in the following discussion, with particular emphasis on the computation of crack tip energy quantities.

3. Elastodynamics

3.1. Linearly elastic materials

For linearly elastic material response, $U = \frac{1}{2}\sigma_{ij}\partial u_i/\partial x_j$ and the stress components have the characteristic inverse square root dependence on radial distance from the crack tip. The dynamic energy release rate $\mathcal{G}$ is proportional to the square of the coefficient of this square root singularity, the so-called elastic stress intensity factor. For a growing crack, the particle velocity also has the inverse square root dependence, whereas the particle velocity vanishes as the square root of the distance from the crack tip for a stationary crack under dynamic loading. The case of dynamic crack growth is considered first.

Consider an arbitrary material area A_o around the crack tip bounded by the curve Γ_o. The curve Γ_o begins on one crack face and ends on the opposite face, as shown in Fig. 1. To be somewhat more precise, A_o is the area enclosed by Γ_o, Γ and the crack faces in the limit as Γ is shrunk onto the crack tip. Application of the divergence theorem to (2.8) leads immediately to the expression,

$$\mathcal{G} = \int_{\Gamma_o}\left(Un_1 - \sigma_{ij}n_j\frac{\partial u_i}{\partial x_1} + \tfrac{1}{2}\rho v^2\frac{\partial u_i}{\partial x_1}\frac{\partial u_i}{\partial x_1}n_1\right)\mathrm{d}\Gamma$$

$$+\int_{A_o}\left(\rho\frac{\partial^2 u_i}{\partial t^2}\frac{\partial u_i}{\partial x_1} - \rho v^2\frac{\partial u_i}{\partial x_1}\frac{\partial^2 u_i}{\partial x_1^2}\right)\mathrm{d}A. \tag{3.1a}$$

At first sight, it might appear that the area integral in (3.1a) is divergent because $\partial u_i/\partial x_1$ and $\partial^2 u_i/\partial t^2$ are singular as $r^{-1/2}$ and $r^{-3/2}$, respectively. This is not so, however, due to the particular combination of terms in the integrand. The displacement gradient near the crack tip has the form $\partial u_i/\partial x_1 = r^{-1/2}f_i(\theta)$ in crack tip polar coordinates, so that the

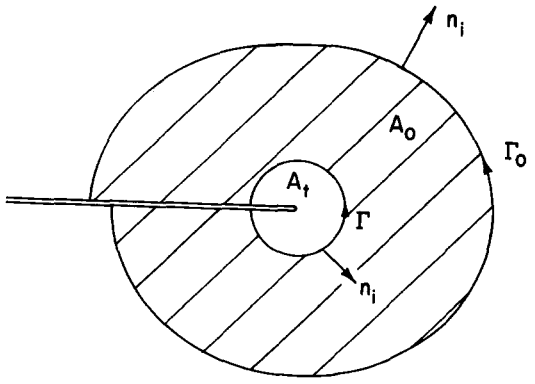

Figure 1. Domain A_o in $x_1 - x_2$ plane is enclosed by Γ, Γ_o and crack faces. A_t is crack tip region enclosed by Γ and crack faces.

second derivative has the form $\partial^2 u_i/\partial x_1^2 = r^{-3/2} g_i(\theta) = -r^{-3/2}[\frac{1}{2} f_i(\theta) \cos\theta + f_i'(\theta)\sin\theta]$. For any angular variation $f_i(\theta)$, it is easily shown that

$$\int_{-\pi}^{\pi} f_i(\theta) g_i(\theta) \mathrm{d}\theta = 0 \tag{3.2}$$

provided that $f_i(\pm\pi)$ is bounded. Thus, the nonintegrable singularity in the area integral in (3.1a) is only apparent and the integral does indeed have a finite value.

While the representation for $\mathscr{G}$ in (3.1a) is certainly correct, it has a feature which is the basis for some concern in considering implementation in finite element procedures. The second term of the integrand in the area integral contains the derivatives of displacement gradients. To obtain non-vanishing second derivatives of the displacements, the elements must have quadratic or higher order interpolation functions for the displacements. Thus, certain classes of elements, including the commonly employed linear displacement elements, are ruled out for such calculations. Furthermore, we note that the products of stress and displacement gradients appear naturally in the virtual work statement of equilibrium and such products can be calculated accurately at the Gauss integration points. However, this accuracy is not preserved for the higher derivatives. Hence, representation (3.1a) may not be ideal for computing the energy release rate.

Other representations for energy release rate may be obtained as follows,

$$\mathscr{G} = \int_{\Gamma_o} \left(U n_1 - \sigma_{ij} n_j \frac{\partial u_i}{\partial x_1} + \tfrac{1}{2}\rho \frac{\partial u_i}{\partial t}\frac{\partial u_i}{\partial t} n_1 \right) \mathrm{d}\Gamma + \int_{A_o} \left(\rho \frac{\partial^2 u_i}{\partial t^2}\frac{\partial u_i}{\partial x_1} - \rho \frac{\partial u_i}{\partial t}\frac{\partial^2 u_i}{\partial x_1 \partial t} \right) \mathrm{d}A \tag{3.1b}$$

$$\mathscr{G} = \lim_{\Gamma \to 0} \int_{\Gamma} \tfrac{1}{2}\rho v^2 \frac{\partial u_i}{\partial x_1}\frac{\partial u_i}{\partial x_1} n_1 \mathrm{d}\Gamma + \int_{\Gamma_o} \left(U n_1 - \sigma_{ij} n_j \frac{\partial u_i}{\partial x_1} \right) \mathrm{d}\Gamma + \int_{A_o} \rho \frac{\partial^2 u_i}{\partial t^2}\frac{\partial u_i}{\partial x_1} \mathrm{d}A. \tag{3.1c}$$

In (3.1c) the first integral is evaluated at the crack tip and the remaining two integrals are evaluated over the finite region. As noted earlier, an accurate evaluation of the integral at the crack tip is virtually impossible to achieve. However, if the contribution from the first integral is small relative to contributions from the other integrals, then (3.1c) could be a useful representation. To pursue this point, note that for linearly elastic fields, the first integral on the right in (3.1c) can be evaluated using the known crack tip field quantities [13] to yield a result which is proportional to the stress intensity factor squared and which depends on the instantaneous crack tip speed. If each term in (3.1c) is divided by $\mathscr{G}$, which is also proportional to the stress intensity factor squared and which depends on the crack tip speed, then the first term on the right in the resulting equation is a function of crack tip speed only. If this speed dependent ratio (denoted by R below) is much smaller than unity, then the first term can be neglected and a relatively simple expression for energy release rate is obtained.

Choosing Γ to be a circular path and using the plane strain relationship between the energy release rate $\mathscr{G}$ and stress intensity factor K given in [13], the ratio R is given by

$$R(v) = \left| \frac{\int_{-\pi}^{\pi} \tfrac{1}{2}\rho v^2 \frac{\partial u_i}{\partial x_1}\frac{\partial u_i}{\partial x_1} n_1 r \mathrm{d}\theta}{(1-\nu^2) A(v) K^2/E} \right|, \tag{3.3}$$

where ν is Poisson's ratio, E is the elastic modulus, K is the elastic stress intensity factor,

and the dimensionless function of speed $A(v)$ is given in [13]. Values of this ratio have been computed using the explicit expressions for angular variation of crack tip fields given in [13]. From the results it is clear that for crack tip speeds smaller than half the shear wave speed, the integral contributes less than 10 percent to the energy release rate, however, the contribution becomes significant at higher crack tip speeds.

With regard to the observation made above, a feature of (3.1b) which is of importance from the point of view of computation is noted. The third and fifth terms in (3.1b) are typically comparable in magnitude but are of the opposite signs, and their net contribution to the energy release rate (i.e. the sum of the two terms) is small. In fact these terms are equivalent to the first term in (3.1c) which has been shown to contribute negligibly to the energy release rate at lower crack tip speed. In other words, a small contribution to the energy release rate is computed from the difference of the two terms of comparable magnitude. This is a potential source of computational error. We conclude that the difference between (3.1b) and (3.1c) is bounded and small for $v/c_2 < 0.5$. The result (3.2) also suggests that the relative contribution from the vicinity of the crack tip to the area integral in (3.1c) is small for uniformly rising loads. Our numerical calculations confirmed this behavior. Hence expression (3.1c) appears to be suited for evaluating the energy release rate from finite element field quantities for crack speeds $v/c_2 < 0.5$.

Finally, it is noted that the expression (3.1c) with $v \to 0$ is exactly the energy release rate expression for the case of a stationary crack subjected to dynamic loads. In this case, the quantity $\mathcal{G}$ must be interpreted as a virtual energy release rate, that is, $\mathcal{G}$ computed from (3.1c) with $v = 0$ is the energy change that would be released if the mechanical fields were frozen at any instant and the crack tip were given an increment of extension in the x_1-direction. Of course, Irwin's relationship between the stress intensity factor and $\mathcal{G}$ holds in this case, and the interpretation of $\mathcal{G}$ as a measure of crack tip field intensity rather than as an energy release rate is more attractive in some respects.

3.2. Nonlinearly elastic materials

All of the energy release rate expressions derived in the preceding section apply for nonlinearly elastic material response, as well as linearly elastic response. However, there are too few theoretical results available for dynamic fracture of nonlinearly elastic materials at the present time to provide a basis for a general discussion. For a stationary crack in a material with a power law stress-strain relationship, it would seem that the near tip fields are adequately described by the HRR asymptotic solution [14,15] provided that their time variation is not too rapid. Analysis of such problems would proceed as in the analysis of certain plasticity problems as considered below in Section 4.

On the other hand, it can be readily shown that a similar separable crack tip asymptotic field cannot be constructed for dynamic growth of a crack in the same material. An indication that analysis of dynamic crack growth in nonlinearly elastic materials may provide some surprises is contained in the recent work reported by Achenbach and Nishimura [16]. They considered the effect of inertia on mode III crack growth in a nonlinearly elastic material for which the effective stress has a constant magnitude for all effective strains greater than a particular level. A principal result is that the total strain remains bounded as the crack tip is approached from a direction directly ahead of the tip. This result poses a dilemma, for it suggests that there may be no energy released at the crack tip although energy continues to flow into the crack tip region from remote points. The resolution of this dilemma may be found through the observation that the material considered admits lines along which displacement gradients are discontinuous [17], and the energy flowing into the crack tip region may be dissipated through propagation of such lines of discontinuity.

4. Elastic-plastic material response

For a stationary crack in a dynamically loaded body of incremental elastic-plastic material, the integral quantity in (2.8) can still be used to some advantage. Of course, the interpretation of the integral as an energy release rate is lost for this case. Nonetheless, it has been demonstrated that if the loading applied to the crack tip region is monotonically increasing and if the stress histories for material particles near the crack tip are nearly proportional, then the value of the integral provides a measure of the intensity of the near tip deformation. It is this role that is pertinent to elastic-plastic fracture mechanics and considerable analytical, numerical and experimental investigations have shown that the values of this integral is a relevant characterizing parameter of the near tip fields of stationary cracks when certain size requirements are met. For dynamic loading conditions and a stationary crack tip, the kinetic energy term T makes no contribution to the integral in (2.8) so that

$$\mathscr{G} = J = \lim_{\Gamma \to 0} \int_{\Gamma} \left(U n_1 - \sigma_{ij} n_j \frac{\partial u_i}{\partial x_1} \right) \mathrm{d}\Gamma, \tag{4.1}$$

where U is a stress work density appropriate for proportional loading of the material. For quasistatic loading conditions and proportional stress history at each material point, the integral in (4.1) is path independent and its value does not depend on a limiting process in which the crack tip contour Γ is shrunk onto the crack tip. In this case, the integral is precisely Rice's J-integral [18], as anticipated in the notation in (4.1). The background for this approach to elastic-plastic fracture mechanics is outlined in recent review articles by Rice [19] and by Hutchinson [20]. In the case of dynamic near tip fields, on the other hand, inclusion of the limit in the definition of J is essential, that is, the J-integral is not path independent under dynamic loading conditions.

Just as in the case of analysis of elastic crack problems by means of computational techniques, the accurate determination of field quantities very near the crack tip is difficult and (4.1) cannot be evaluated directly. Application of the divergence theorem, however, leads to the alternate form

$$J = \int_{\Gamma_o} \left(U n_1 - \sigma_{ij} n_j \frac{\partial u_i}{\partial x_1} \right) \mathrm{d}\Gamma + \int_{A_o} \rho \frac{\partial^2 u_i}{\partial t^2} \frac{\partial u_i}{\partial x_1} \mathrm{d}A, \tag{4.2}$$

where the path Γ_o and the area A_o are as shown in Fig. 1. An illustration of the form (4.2) will be presented in the following section. Even in the case of dynamic growth of a crack in an incremental elastic-plastic material, the integral (2.8) can be applied for an appropriate definition of the term U. It has not been found to be particularly useful, however, because the near tip fields for growing cracks tend to be less singular than the corresponding fields for stationary cracks and the value of $\mathscr{G}$ is then zero. The physical interpretation of this result is that all of the energy that flows into the crack tip region is either dissipated through plastic flow or is trapped as residual elastic energy in the wake of the crack tip plastic zone.

An exception to this situation arises for rate-dependent plastic response when the rate sensitivity is sufficiently pronounced. A problem of a crack growing at high speed in an elastic/rate-dependent plastic solid under small scale yielding conditions was considered by Freund and Hutchinson [21]. At high stress levels, such as those that arise near the tip at high crack speed, it was assumed that the plastic strain rate increases linearly with stress. In this case, the near tip fields are sufficiently singular to result in a finite value for $\mathscr{G}$ in (2.8), and a general expression is derived in [21] for the near tip energy release rate in terms of the overall release rate for steady growth. In fact, for steady state growth, the integral in (2.8) is path independent for general material response [6,21].

5. Finite element analyses of stationary and propagating cracks

5.1. Elastodynamic analysis

Computational aspects of the domain integral representations for the energy release rate as given in Section 3 are discussed in this section. To emphasize the interpretation of these energy integrals (3.1) as a measure of the crack tip field intensity, the symbol J will be employed in place of $\mathscr{G}$ hereafter. In (3.1) the domain A_o is enclosed by Γ_o, Γ and the crack faces in the limit as Γ is shrunk onto the crack tip. From result (3.2), it is clear that the contributions from the area integrals in (3.1) taken over the domain A_t (indicated in Fig. 1) as Γ is shrunk onto the crack tip must vanish. Hence in the context of numerical integration A_o will be taken to be the entire area enclosed by Γ_o and the crack faces. The energy integrals have the form given in (3.1), of course.

The numerical studies were carried out with the finite element program ABAQUS [22]. The Hilber–Hughes–Taylor algorithm [23] is employed to integrate the semi-discrete equation of motion. A small amount of damping is invoked by setting the α value to be -0.05. Both 4-noded bilinear isoparametric element and 8-noded biquadratic isoparametric element are used in the calculations. Unless otherwise stated, element stiffness matrices are obtained by 2×2 Gaussian integrations.

To indicate the implementation of these energy integrals in our finite element calculations, the discrete form of (3.1b) is given as follows

$$J = \sum_{\text{all segments on } \Gamma_o} \sum_{i=1}^{2} w_i \left[\left(U - \sigma_{11} \frac{\partial u_1}{\partial x_1} - \sigma_{21} \frac{\partial u_2}{\partial x_1} + \tfrac{1}{2}\rho \frac{\partial u_1}{\partial t} \frac{\partial u_1}{\partial t} + \tfrac{1}{2}\rho \frac{\partial u_2}{\partial t} \frac{\partial u_2}{\partial t} \right) P_2 + \left(\sigma_{12} \frac{\partial u_1}{\partial x_1} + \sigma_{22} \frac{\partial u_2}{\partial x_1} \right) P_1 \right]_i + \sum_{\text{all elements in } A_o} \sum_{i=1}^{4} w_i \left[\left(\rho \frac{\partial^2 u_1}{\partial t^2} \frac{\partial u_1}{\partial x_1} + \rho \frac{\partial^2 u_2}{\partial t^2} \frac{\partial u_2}{\partial x_1} - \rho \frac{\partial u_1}{\partial t} \frac{\partial^2 u_1}{\partial x_1 \partial t} - \rho \frac{\partial u_2}{\partial t} \frac{\partial^2 u_2}{\partial x_1 \partial t} \right) D \right]_i . \tag{5.1}$$

Here P_1 and P_2 are the path factors given in [24], w_i are the appropriate Gauss weights and all quantities within $[\ ]_i$ are evaluated at the respective Gauss points. Also D is the determinant of the Jacobian matrix of the isoparametric transformation. Similar discrete expressions can be written for (3.1a) and (3.1c). A more detailed discussion of a discrete representation for a domain integral representation for the dynamic J can be found in [25].

The dynamic J-integrals (3.1) are independent of the size of the domain A_o enclosed by the contour Γ_o as indicated in Fig. 1. This invariant feature of the domain integrals can serve as a useful check on the self-consistency of the numerical calculations. As noted previously, accurate finite element solutions for points near the crack tip are difficult to obtain. Hence the domains of integrations typically extend over ten or more elements.

To evaluate the computational aspects of the numerical algorithm and of the energy integrals, a stress wave problem with an exact solution is employed as the benchmark problem. Freund [26] considered a semi-infinite crack in an infinite plane subjected to a tensile stress wave normal to the crack plane. At $t = 0$, the stress wave arrives at the crack plane and at a later time, $t = \tau$, the crack starts to propagate. The analytical solution for the dynamic stress intensity factor in the interval $0 < t < \tau$ (i.e., the crack is stationary) is

$$K(t) = B\sigma_a \sqrt{c_1 t}\,. \tag{5.2}$$

Here c_1 is the longitudinal wave speed for the medium, σ_a is the magnitude of the tensile pulse with step function time dependence and B is a function of Poisson's ratio given in [26]. For times $t > \tau$, the dynamic stress intensity factor for the propagating crack is

$$K(t, v) = k(v) B \sigma_a \sqrt{c_1 t}, \tag{5.3}$$

where v is the crack tip speed and $k(v)$ is defined in [27] as a function which decreases monotonically from one at $v = 0$ to zero when v is the Rayleigh wave speed.

For the purpose of comparison with numerical results presented subsequently, the well known relation between the dynamic J and the dynamic stress intensity factor under plane strain condition is given by

$$J(t, v) = \frac{(1 - \nu^2)}{E} A(v) [K(t, v)]^2. \tag{5.4}$$

Here $A(v)$ is a universal function of crack tip speed [13]. For a stationary crack ($v = 0$), A is unity, and A increases monotonically with increasing v. In the subsequent analyses, ν is taken to be 0.3.

5.2. Elastic analysis of a stationary crack subject to a single step pulse

A step pulse is applied at $t = -H/c_1$ at the edge $x_2 = H$ of the model shown by inset in Fig. 2, and the pulse arrives at the crack plane at $t = 0$. Since the problem has no reflective symmetry with respect to the crack plane ($x_2 = 0$ plane), the domain downstream from the crack plane is included in the model. To simulate the infinite plane problem for which the solution (5.2) is applicable, the dimension H must be large enough so that within the period of interest, reflected waves from the boundaries do not reach the vicinity of the crack tip. In addition the length of the model (in x_1-direction) must be sufficiently large compared to H so that within the interval of interest, the crack tip region is unaffected by the unloading waves emanating from the remote edges. These factors were taken into consideration in selecting the dimensions of the finite element model. The full plane model constructed with 8-noded elements has 200 elements (10 by 20 arrangement) and 681

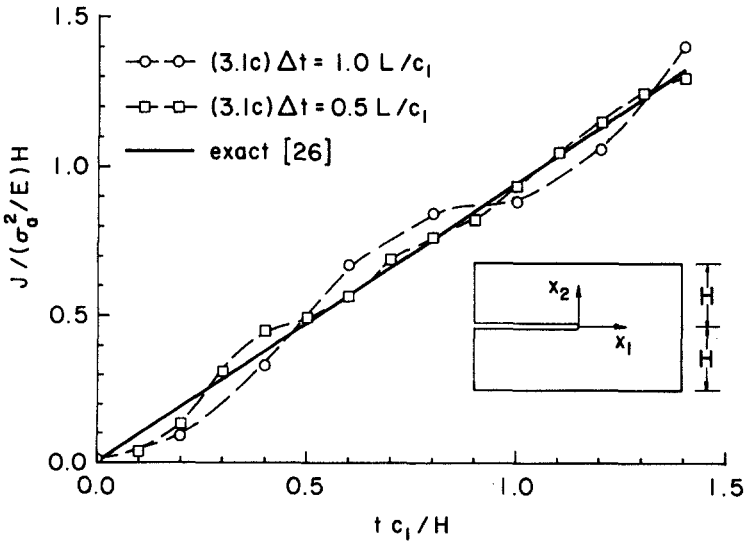

Figure 2. Variation of normalized J with normalized time as determined from the full plane model. Results obtained from two analyses using different time steps and the exact solution are shown. Shown in inset is a schematic of the full plane model and the fixed reference coordinates x_1 and x_2.

nodes. All elements are square shaped and are identical in size with the length (and width) being L. The time required for a longitudinal wave to traverse an element is then L/c_1.

Two calculations were carried out; the first employs uniform time steps of $\Delta t = 1.0L/c_1$ and the second employs uniform time steps of $\Delta t = 0.5L/c_1$. At the end of each time step, the dynamic J is computed from the stress and deformation fields using the discrete representation of (3.1c). Typically the dynamic J is evaluated on ten integration domains; the smallest domain has 4 elements and the largest domain has 200 elements. With the exception of the near-tip domain, which has four elements, the values of J evaluated on the other domains are within one percent of its mean value which attest to the consistency of the numerical solution. The dynamic J values determined from an alternate representation (3.1b) are also in agreement with the values determined from (3.1c). This provides an additional check on the consistency of the results. In subsequent discussions, the mean of the domain values will be reported as the dynamic J.

The dynamic J computed from (3.1c) is shown in Fig. 2 together with the exact solution (5.2) expressed in terms of J through (5.4). The computational solution clearly converges to the exact solution for the smaller time step. At sufficiently large times, say $t > 0.5H/c_1$, the finite element results for the smaller time step is within three percent of the exact solution. At shorter times, the error is substantially larger. This is not unexpected since at short times the refracted wave from the crack tip has traveled through relatively few elements (i.e., small domain), and as previously discussed, an accurate evaluation of the dynamic J in this case is rather difficult.

Similar calculations were also carried out using a mesh where the crack tip region is comprised of regular triangular and singular triangular elements [28]. Solutions from these models and from a model comprised solely of 4-noded elements (the latter model has 800 elements) are in substantial agreement with the numerical results shown in Fig. 2. Solutions from these models are also exhibit the same convergence characteristics described above. It is clear from this numerical study that (3.1c) and (3.1b) are suited for the determination of the dynamic J using field quantities obtained from finite element analysis.

5.3. Elastic analysis of a stationary and propagating crack subject to symmetrically applied step pulses

A computational analysis of crack propagation requires a finite element model which is substantially larger than the models employed in the preceding section for the stationary crack analysis. To reduce the size of the computational problem we consider a cracked plate symmetrically loaded by tensile step pulses on the edges $x_2 = \pm H$. Since this problem possesses reflective symmetry with respect to the crack plane, only the upper half plane needs to be considered. The solutions (5.2) and (5.3) are still applicable to this problem and by superposition, the magnitude of the dynamic K is twice that for the single step pulse.

For this analysis the upper half plane is modelled by 4-noded isoparametric elements. This choice is guided by our numerical experimentations on dynamically propagating cracks which indicate that the node release technique is better suited with 4-noded elements. The upper half plane model has 1290 elements (15 by 86 arrangement) and 1392 nodes. All elements are square shaped and identically sized. Homogeneous displacement boundary conditions are prescribed on the symmetry plane $x_2 = 0$, $x_1 \geq 0$.

To compare the convergence characteristics for the half plane model with the full plane model of the preceding section, calculations similar to those reported in Section 5.2 were carried out for a stationary crack. The convergence behavior with respect to element size and time steps for the present model is similar to that described in Section 5.2.

Nevertheless the results from the full plane model are in better agreement with the exact solution when equivalent meshes and identical time steps are employed. The solution obtained from the half plane refined mesh model (as described in the preceding paragraph) with uniform time steps of $0.25L/c_1$ and the exact solution are shown in Fig. 3. For $t > 0.2H/c_1$; the dynamic J agreed very well with the exact solution.

Before describing the main results, the algorithm for extending the crack is briefly discussed. Consider a crack propagating at constant speed v. The time required for the crack advance through one element length is L/v and denoted by t_e. At the start of the crack advance, the zero displacement boundary condition at the crack tip is replaced by an equivalent concentrated force, F_o, required to maintain the prescribed displacement. The nodal force is relaxed to zero in following increments according to a so-called "constant energy release rate" [29,30] relation,

$$F(t) = F_o\sqrt{1 - t/t_e}, \tag{5.5}$$

where t is the time elapsed from the start of the node release and $F(t)$ is the nodal force at time t. The merits of this nodal force relaxation scheme and other node relaxation schemes are discussed in [30]. We experimented with several nodal force relaxation schemes on several benchmark problems and reached the conclusion that the scheme according to (5.5) gave dynamic J results which are consistent with analytical solutions.

The problem to be analyzed is as follows. At time $t = -H/c_1$ a step pulse is applied at $x_2 = H$, and the longitudinal wave reaches the crack plane at $t = 0$. The crack tip is stationary for $t < \tau$, and it propagates at a constant speed v for $t \geq \tau$. Within the interval $-H/c_1 < t < \tau$, the calculations employ uniform time steps of $\Delta t = 0.25L/c_1$, where L/c_1 is the time required for the longitudinal wave to travel through an element. For $t \geq \tau$ the time steps are governed by the speed of the propagating crack v and the element size L. The crack advances across an element boundary (on $x_2 = 0$) in 20 increments, and this corresponds to uniform time steps of $\Delta t = L/20v$. The analyses were carried out for crack tip speeds of $0.4c_2$ and $0.6c_2$ respectively, where c_2 is the shear wave speed.

In the first analysis, the crack is stationary between $-H/c_1 < t < 0.467H/c_1$ and then prescribed to propagate at a uniform speed of $0.4c_2$. For the model employed, the time span where the numerical solution pertains to the semi-infinite crack in an infinite plane

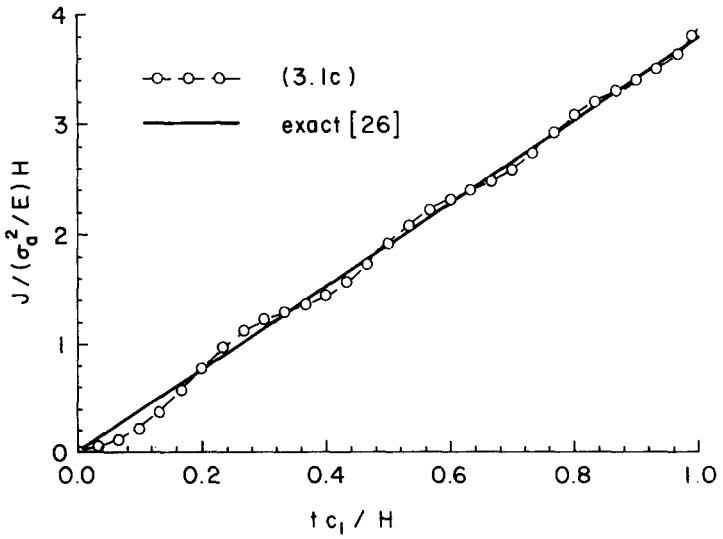

Figure 3. Comparison of normalized J as determined from the half plane model with the exact solution.

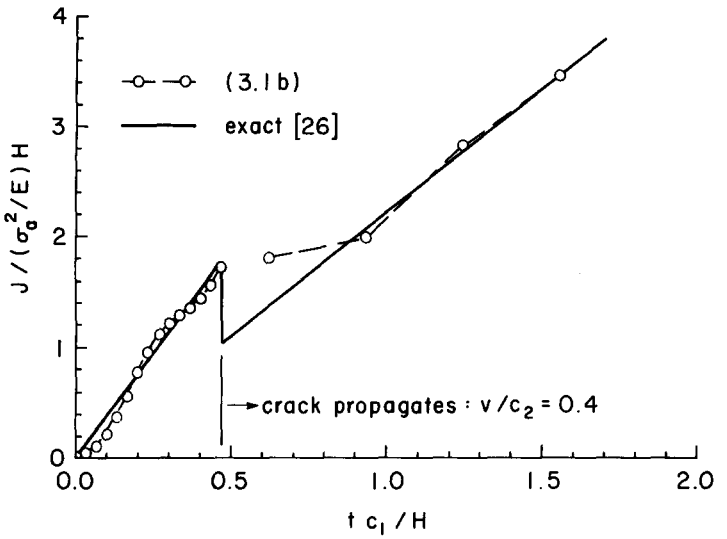

Figure 4. Comparison of normalized J with the exact solution. Crack propagates at speed $v/c_2 = 0.4$ at $t > 0.467H/c_1$.

problem is $-H/c_1 < t < 2H/c_1$. During this interval the crack tip advanced through four nodes. The dynamic J is evaluated at every time step. For $t < 1.667H/c_2$, the dynamic J values evaluated on various domains using (3.1b) are within several percent of its mean value. Thus the numerical results are consistent with the domain independence of the dynamic J integral. At longer times, the values become domain dependent and we attribute this to the dispersion of the waves reflected from the boundaries and numerical errors associated with the node release technique. The average of the dynamic J associated with each unloading process is shown in Fig. 4. Within the interval indicated, the numerical results agreed reasonably well with the exact solution.

Numerical results of the dynamic J for the crack propagating at $v = 0.6c_2$ are shown in Fig. 5. Here τ is set at $0.467H/c_1$ and the crack tip advanced through six nodes within the

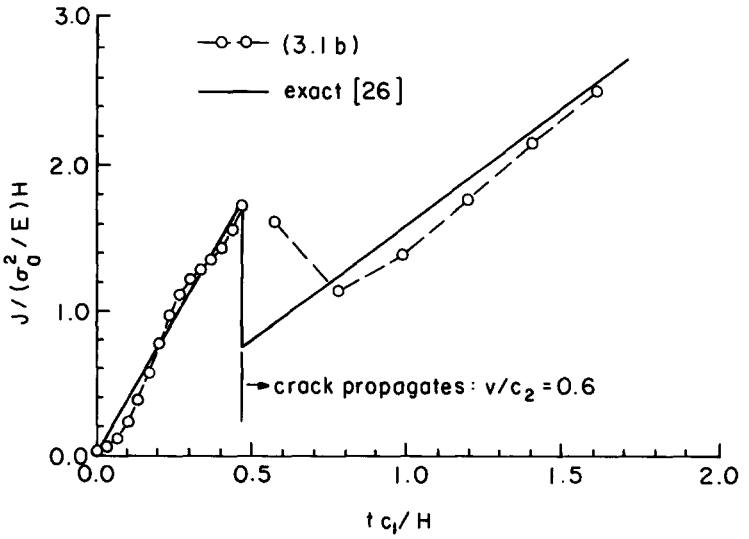

Figure 5. Comparison of normalized J with the exact solution. Crack propagates at speed $v/c_2 = 0.6$ at $t > 0.467H/c_1$.

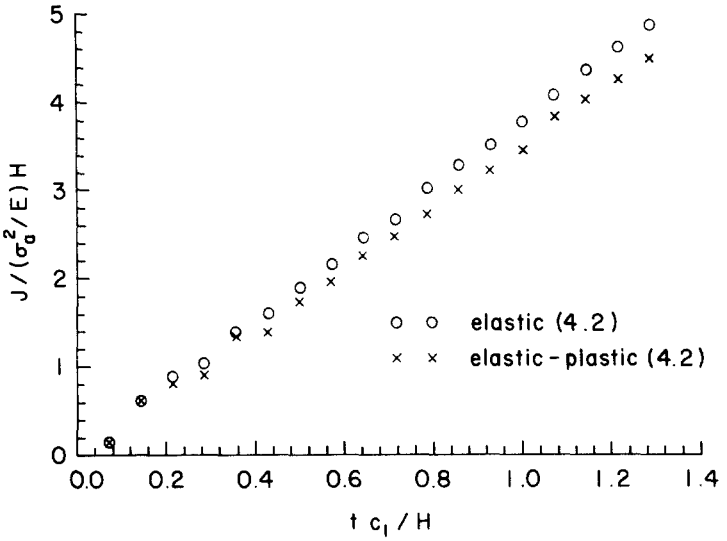

Figure 6. Behavior of dynamic J with respect to time as determined from elastic and elastic-plastic analyses.

period of interest. Again, the agreement between numerical results and the exact solution is reasonably good. It should be noted that the error expressed in terms of the dynamic stress intensity factor is only half of that for the dynamic J.

5.4. Elastic-plastic analysis of stationary crack subject to symmetrically applied step pulses

An elastic-plastic dynamic analysis is carried out using the half configuration discussed in Section 5.3 based on the following uniaxial tensile stress-strain relation,

$$\epsilon/\epsilon_o = \sigma/\sigma_o, \qquad \epsilon < \epsilon_o$$
$$\epsilon/\epsilon_o = (\sigma/\sigma_o)^n, \qquad \epsilon \geq \epsilon_o. \tag{5.6}$$

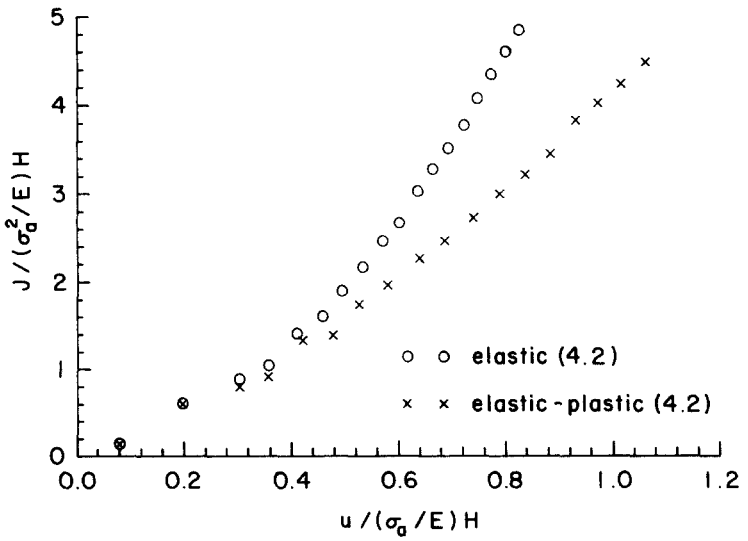

Figure 7. Behavior of dynamic J with respect to crack tip opening displacement as determined from elastic and elastic-plastic analyses.

Here n is the strain-hardening exponent, ϵ_o and σ_o are reference strain and stress related by $\sigma_o = E\epsilon_o$. In this particular study n has a value of 10 which corresponds to a lightly hardening material. The relation (5.6) is generalized to multiaxial stress states according to a J_2 flow theory of plasticity.

Elastic-plastic dynamic calculations were carried out for a mesh comprised of only 4-noded elements and another mesh comprised of only 8-noded elements. The results from both calculations are very similar and we restrict the discussion to results obtained from the 8-noded element model. The half plane model has 456 elements (12 by 38 arrangement) and 1469 nodes. Elements near the crack tip are square shaped and identically sized. Larger elements are employed at further distances from the crack tip. Symmetry conditions, that is, zero displacement boundary conditions are prescribed on the crack plane $x_2 = 0$ and $x_1 \geqslant 0$. A tensile step load σ_a of magnitude $0.6\sigma_o$ is applied on the boundary at $x_2 = H$. Uniform time steps of $0.5L/c_1$ where L is the size of the square elements in the vicinity of the crack tip is employed throughout the calculations. The calculation is terminated when the reflected waves from the boundaries reach the plastic zone emanating from the crack tip.

The dynamic J is computed according to (4.2). In this case the integration of the stress work density U follows the actual strain trajectory of a material point. (For a stationary crack, (3.1c) is identical to (4.2) if U in (3.1c) is taken to be the stress work density.) Again we observed that values evaluated on differently sized domains are within one percent of the main value throughout the entire analysis. This lends confidence to this particular elastic-plastic dynamic solution. The rise of dynamic J with respect to time is shown in Fig. 6. To gauge the effect of plasticity, we have included in the figure the elastodynamic J obtained from the same mesh using the identical time steps. The behavior of the dynamic J with respect to the opening displacement of the node at a distance L behind the crack tip as determined from the elastic and elastic-plastic analyses are shown in Fig. 7. The trend of these solutions are in accord with quasi-static results. An analytical solution to this problem is not available and more definite statements concerning the accuracy of the elastic-plastic numerical solution cannot be made. Nevertheless, results from another study [25] do provide information which is pertinent to the present discussion. In that study, a deeply notched round bar was subjected to a tensile pulse with a wave length which is long compared to the bar diameter. The dynamic J obtained from (4.2) agreed well with the values determined from a deep crack formula based on the remote load and displacement [31]. These earlier comparison taken together with the present results indicate that finite domain integrals can be employed to extract accurate values of the dynamic J from finite element solutions.

Acknowledgements

We gratefully acknowledge the research support of the Naval Sea Systems Command (SEA 05R15) through NBS Grant NB82RA20004, the National Science Foundation through Grant MEA82-10931, and the NSF Materials Research Laboratory at Brown University through Grant DMR83-16893.

The calculations described here were performed in the VAX-11/780 Computational Mechanics Facility at Brown University. This facility was made possible by grants from the National Science Foundation (Solid Mechanics Program), the General Electric Foundation, and the Digital Equipment Corporation.

References

[1] C. Atkinson and J.D. Eshelby, *International Journal of Fracture Mechanics* 4 (1968) 3–8.
[2] B.V. Kostrov and L.V. Nikitin, *Archiwum Mechaniki Stosowanej* 22 (1970) 749–775.
[3] L.B. Freund, *Journal of Elasticity* 2 (1972) 341–349.
[4] L.E. Malvern, *Introduction to the Mechanics of a Continuous Medium*, Prentice-Hall (1969) 210–211.
[5] J.D. Eshelby, in *Inelastic Behavior of Solids*, edited by M.F. Kanninen et al. McGraw-Hill (1970) 77–115.
[6] J.R. Willis, *The Mechanics and Physics of Fracture*, The Metal Society (1975) 57–67.
[7] K. Kishimoto, S. Aoki and M. Sakata, *Engineering Fracture Mechanics* 13 (1980) 387–394.
[8] S. Aoki, K. Kishimoto and M. Sakata, *Engineering Fracture Mechanics* 20 (1984) 827–836.
[9] S.N. Atluri, *Engineering Fracture Mechanics* 16 (1982) 341–364.
[10] T. Nishioka and S.N. Atluri, *Engineering Fracture Mechanics* 18 (1983) 1–22.
[11] T. Nishioka and S.N. Atluri, *Engineering Fracture Mechanics* 18 (1983) 23–33.
[12] T. Nishioka and S.N. Atluri, *AIAA Journal* 22 (1984) 409–414.
[13] L.B. Freund, in *Mechanics Today, Vol. III*, edited by S. Nemat-Nasser, Pergamon (1976) 55–91.
[14] J.W. Hutchinson, *Journal of the Mechanics and Physics of Solids*[15 16 (1968) 13–31.
[15] J.R. Rice and G.F. Rosengren, *Journal of the Mechanics and Physics of Solids* 16 (1968) 1–12.
[16] J.D. Achenbach and N. Nishimura, "Effect of inertia on finite near tip deformation for fast mode III crack growth", *Journal of Applied Mechanics* (to appear).
[17] J.K. Knowles and E. Sternberg, *Journal of Elasticity* 10 (1980) 81–110.
[18] J.R. Rice, *Journal of Applied Mechanics* 35 (1968) 379–386.
[19] J.R. Rice, in *Proceedings of the 8th US National Congress of applied Mechanics*, edited by R.E. Kelley, Western Periodicals, No. Hollywood, CA (1979) 191–216.
[20] J.W. Hutchinson, *Journal of Applied Mechanics* 50 (1983) 1042–1051.
[21] L.B. Freund and J.W. Hutchinson, "High strain-rate crack growth in rate dependent plastic solids", *Journal of the Mechanics and Physics of Solids* (to appear).
[22] ABAQUS, Hibbitt, Karlsson and Sorenson, Inc., Providence, Rhode Island.
[23] H.M. Miller, T.J.R. Hughes and R.L. Taylor, *Earthquake Engineering and Structural Dynamics* 5 (1972) 129–140.
[24] C.F. Shih and A. Needleman, *Journal of Applied Mechanics* 51 (1984) 48–56.
[25] T. Nakamura, C.F. Shih and L.B. Freund, "Elastic plastic analysis of a dynamically loaded circumferentially notched round bar", *Engineering Fracture Mechanics* (to appear).
[26] L.B. Freund, *Journal of the Mechanics and Physics of Solids* 21 (1973) 47–61.
[27] L.B. Freund, *Journal of the Mechanics and Physics of Solids* 20 (1972) 129–140.
[28] R.S. Barsoum, *International Journal on Numerical Methods in Engineering* 11 (1977) 85–98.
[29] G. Rydholm, B. Fredriksson and F. Nilsson, in *Numerical Methods in Fracture Mechanics*, edited by A.R. Luxmoore and D.R.J. Owens, University of Swansea, Swansea, Wales (1978) 660–672.
[30] J.F. Malluck and W.W. King, in *ASTM STP* 711, American Society for Testing and Materials (1980) 38–53.
[31] J.R. Rice, P.C. Paris and J.G. Merkle, in *ASTM STP* 536, American Society for Testing and Materials (1973) 231–245.

Résumé

On passe en revue les développements dans l'utilisation de l'intégrale du flux d'énergie à l'extrémité d'une fissure dans le calcul de la mécanique de la rupture dynamique et ce, au cours des 5 dernières années. On en tire une expression du flux d'énergie à l'extrémité d'une fissure en fonction du champ mécanique au voisinage de cette extrémité, expression applicable aux réactions générales d'un matériau. On démontre ensuite que certaines intégrales d'énergie intéressantes peuvent être extraites des résultats généraux en mettant en exergue les caractérisations adéquates de la réponse du matériau. Diverses représentations alternatives du flux d'énergie sous forme d'intégrale couvrant certaines régions finies autour de l'extrémité de la fissure sont présentées et comparées, en vue d'une insertion dans des études de simulation per éléments finis.